

Balancing CO_2 Emissions and Economic Cost in a Microgrid through an Energy Management System using MPC and Multi-Objective Optimization

Luis O. Polanco Vásquez[a], Juana López Redondo[b], José Domingo Álvarez Hervás[b], Víctor M. Ramírez[a,*], José Luis Torres[b]

[a] *Unidad de Energía Renovable, Centro de Investigación Científica de Yucatán AC, luis.polanco@cicy.mx, victor.ramirez@cicy.mx, Mérida, 97205, Yucatán, México*
[b] *University of Almería, Agrifood Campus of International Excellence (ceiA3) CIESOL Joint Centre University of Almería-CIEMAT, jlredondo, jhervas, jltmoreno@ual.es, Almería, 04120, Almería, Spain*

Abstract

In this work, the energy production of a microgrid is managed to satisfy the demand while simultaneously minimizing two objectives: CO_2 emissions and the economic cost of operating the microgrid. To this end, a novel energy management system (EMS) that combines a Model Predictive Control (MPC), a multi-objective optimization algorithm and a decision-tool, has been developed. This EMS takes advantage of the individual strengths of these components to address the changes that frequently appear in the microgrid operating conditions. Unlike traditional optimization, MPC applies the concept of receding horizon, so that the optimization problem covers a prediction horizon instead of the entire simulation time. In addition, it is rerun at each simulation sample time with updated information, so that the controller can adapt to changes. The multi-objective optimization algorithm optimizes the CO_2 emissions and the economic cost (these two objectives are in conflict objectives and need to be optimized simultaneously) and generates a set of solutions, each of which is a trade-off between the two objectives. These solutions are called Pareto optimal solutions, and they form the Pareto front. The decision-tool automates the process by managing the Pareto front obtained from the multi-objective optimization. It acts as an expert and selects, among those equally suitable solutions, the one that best

*Corresponding author

fits the current priorities. To test the performance and robustness of the MPC and to demonstrate that the decreasing horizon actually helps to mitigate the uncertainties in the predictions, two simulations are performed. In the first one, the forecasting variables are assumed to be predicted without errors, while in the second one, a prediction error is added to these variables. For each experiment, the decision-tool has been adjusted to select, from the Pareto front provided by the multi-objective algorithm, different solutions satisfying various requirements.

Keywords:
Model Predictive Control, Multi-objective optimization, Decision-tool, CO_2 Emissions Minimization, Economic Cost Minimization, Energy Management System, Changing Operating Conditions, Trade-off Solutions

---

1. Introduction

In global markets reference indices, the rise in certain fossil fuels, such as gas and oil, is putting pressure on the price of electricity in most countries' electricity markets [1]. This increase is due to several factors that are not necessarily mutually exclusive: i) the fact that the production peak of the main gas suppliers may have been reached [2]; ii) various geopolitical tensions affecting supply, such as the war in Ukraine; and, iii) logistical and transportation problems due to the upturn in energy demand once the pandemic caused by Covid-19 is behind us. These factors are accelerating the energy change from a model dependent on fossil fuels, which are limited, polluting and in the hands of a few countries, to another energy model in which renewable energies cover, if not all, a significant part of energy demand. Within this framework, microgrids emerge as a new type of electrical grid based on renewable energies, which incorporate a control system that also seeks to maximize energy use from these sources.

Today, microgrids are an essential element within electricity distribution systems. They are also a technically feasible solution to reduce CO_2 emissions. Within microgrids, the control system is a key element, as they allow the integration of renewable energy sources and storage in point-of-use energy systems. Among other controllers, Model Predictive Control (MPC) is a suitable control scheme due to its ability to include demand forecasts, weather conditions, and renewable energy production. In addition, MPC allows direct optimization of incentives such as CO_2 emissions, electricity to the main grid, or monetary costs (known as economic MPC). Most of the works presented in the literature have addressed the optimization of one of these objectives, either using heuristic optimization techniques or with deterministic algorithms. However, when more than one objective has been considered simultaneously, the multi-objective problem has often been reduced to a constrained single-objective optimization problem [3]. Nevertheless, as stated in [4], multi-objective optimization has many advantages over single-objective optimization for energy management in microgrids. For example, the multi-objective solution offers many more trade-off solutions, eligible according to the different constraints provided by the decision tool methodology. The computation time is also more advantageous, since almost the same time is used to obtain more solutions than in a single-objective problem. This methodology is perfect for cases where microgrids are scalable and/or conditions change rapidly [5]. Therefore, there is a need for a systematic approach and formalizing a multi-objective optimization problem [5].

In this context, the contribution of this work is twofold. On the one hand, it proposes an EMS that combines a stochastic multi-objective optimization with an MPC to help mitigate the uncertainties introduced by renewable energy in microgrids. On the other hand, it uses an automatized decision tool to select, among the available ones, the most suited solution for the current conditions.

Integrating multi-objective optimization with stochastic methods to improve predictions in the variations introduced by renewable energies, specifically solar and wind, is not widely studied in the literature. As far as we know, only in [6] an optimization model with probabilistic constraints is proposed to improve the generation predictions of renewable systems. In fact, only a few works seek to improve energy management by integrating techniques such as MPC, fuzzy control and modern control techniques in multi-objective optimization [5, 7, 8]. In this work, we opt for an MPC since it is a widely used industrial control scheme that internally uses a model of the system to be controlled. The MPC monitors the control of a microgrid and can predict weather conditions or renewable energy production over a predefined horizon. Finally, it also includes a method that can optimize one or several objective functions, depending on the problem. This paper considers the energy cost and the emissions produced by fossil fuels, resulting in a bi-objective optimization problem.

Apart from a few works such as [9], most studies in the microgrids literature propose the optimization of bi-objective problems [5, 7, 8, 10, 11].

More precisely, in [9], a multi-objective analysis of more than two criteria for microgrids is performed, taking into account the social approach that is very important nowadays for the business environment. The rest of the articles mainly focus on minimizing energy cost optimization by managing the renewable generation and operating costs of different energy sources as one of the objective functions. The second objective varies depending on the work considered. For example, works [8, 10] optimize the energy availability due to the intermittency of both solar photovoltaic and wind systems by managing the storage systems, i.e., implicitly minimizing the degradation rate of these systems. The work [11] considers the minimization of the environmental pollution rate as a second objective, and the works [5, 12] optimize the thermal comfort for systems that include heat or cooling generation by internal combustion engines using biogas and other fuels.

Solving a multi-objective optimization problem is not a mean task. To deal with it, a genetic algorithm has been considered here. These methods can find multiple optimal solutions in a single simulation run due to its population-based search approach [13]. Additionally, they are demonstrated to be suitable to deal with related optimization problems as [8, 10, 11, 14, 15, 16, 17, 18]. As a result, the multi-objective method does not provide a single solution that simultaneously minimizes all objective functions. Instead, the solution consists of several trade-off points in the feasible space known as the Pareto front [19]. This paper also proposes an online decision tool that selects the preferable point, according to some pre-specified requirements, without the intervention of an expert. This idea of selecting the best solution needs to be explored more profoundly in the microgrids framework, i.e. only a few papers include the concept of decision maker in the study [10], while others present an analysis of the metrics and normalization schemes to select inflexion points of the Pareto front [5].

Finally, to conclude with the review of this topic, we highlight some works where the storage system of the microgrid is coordinated through a cloud platform, and the monitoring of the operation of the battery pack is carried out in real-time [20, 21, 22].

The paper is organized into the following sections: in Section 2, the proposed EMS is presented, both the MPC controller and the model are described, and the particular optimization problem for our microgrid as well as the decision tool are shown. Section 3 shows the case studies and verification of the simulation results. Finally, section 4 presents the main conclusions drawn from this work.

2. Energy management system

As pointed out before, this work proposes an EMS with a unifying framework between multi-objective optimization and MPC. Figure 1 shows a representation of the implemented scheme. In the following, the important components of the designed scheme are deeply explained.

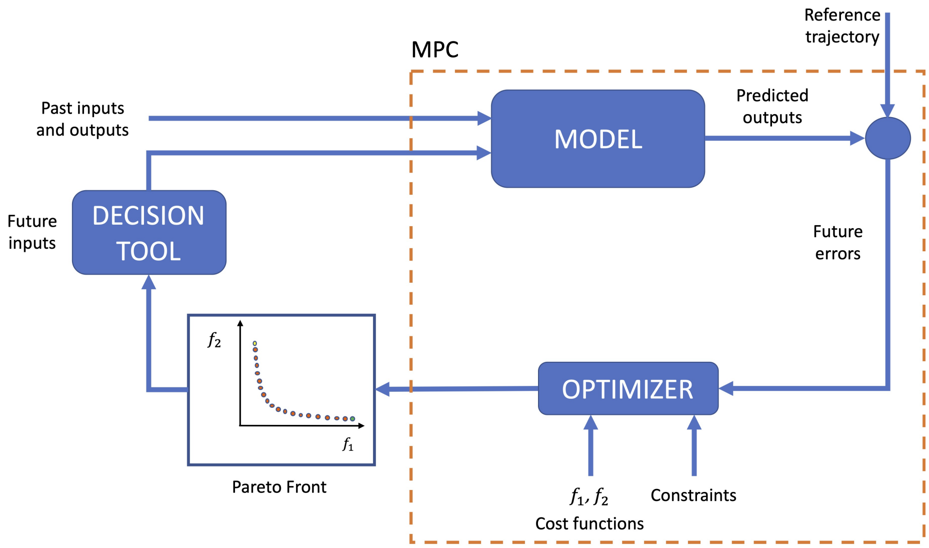

Figure 1: Implemented EMS scheme.

2.1. Model-based Predictive Control

Generally speaking, MPC is based on the iterative and finite-horizon optimization of a plant model. At time t, the current output $y(t+1)$ of the plant is predicted using a model of the process, and a control strategy $u(t+1)$ that optimizes the cost function is computed for a relatively short future time horizon, N_p. Specifically, an online or on-the-fly calculation is used to explore state trajectories arising from the current state and to find a cost-optimized control strategy up to the time $(t+N_c)$, where N_c is the control horizon. Only the first step of the control strategy is implemented. The state of the plant is sampled again, and all calculations are repeated based on the new current state, giving rise to further control and new predictions in the state path $v(t+1)$. The prediction horizon is constantly updated forward and, for this reason, it is said that the MPC has the feature of receding control horizon [23] (see Figure 2).

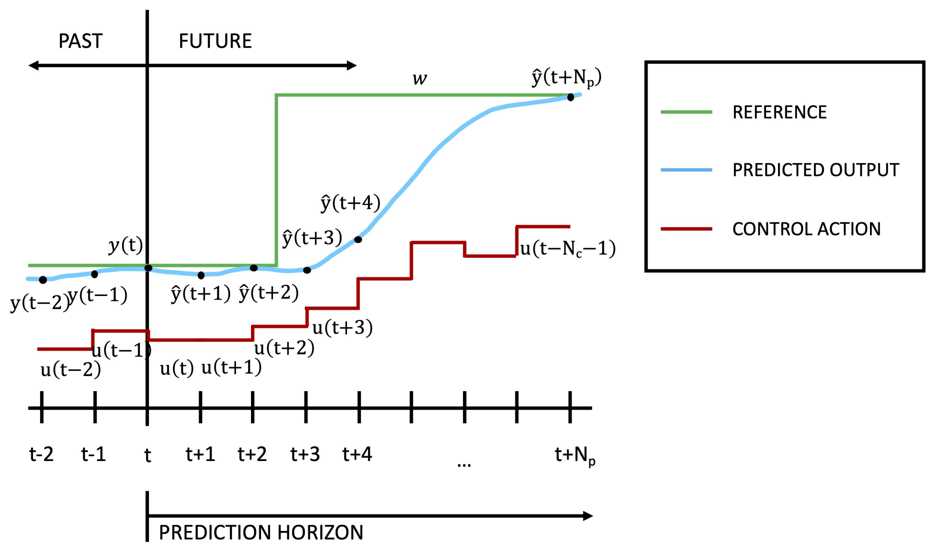

Figure 2: Representation of the receding control horizon in an MPC.

2.2. Model

The mathematical models used for the microgrid components in this work are briefly described in this section. The connection to the main grid is modelled as a Point of Common Coupling (PCC), which is electrically robust and is used for unlimited exchange of active and reactive power. The PCCs are modelled as generation sources that operate at voltage levels within limits given by the electrical system, as shown in Equation 1. Another essential element in the microgrid is the storage system; it is modelled as a system that consumes energy $P_{Bcj} < 0$ when it is charging and as a source that delivers energy to the microgrid $P_{Bdj} > 0$ when the system is dischargin (see Equation 2); in addition, the State Of Charge (SOC) of the storage system can be approximated by Equation 3 for any instant t. The wind system is modelled as an uncontrolled source of active power that depends on the speed of the wind S_w, its density δ_w and the area covered by its blades A_w (see Equation 4). The model used for the photovoltaic system is widely known as model of one diode, Equation 5 describes the behaviour of the power generated by the PV as a function of the terminals current and voltage. The PV terminal voltage and current equations are described in detail in [24]. The diesel generator is modelled as a system that delivers minimum and maximum power at appropriate voltage levels. The load model represents the constant power for the entire time interval T. Equation 6 describes it.

$$\left\{\underline{V}_j \leq V_j^{t_k} \leq \bar{V}_j; \underline{\theta}_j \leq \theta_j^{t_k} \leq \bar{\theta}_j\right\} \forall t_k \in T \tag{1}$$

$$P_{Bnj}^{t_k} = P_{Bcj}^{t_k} + P_{Bdj}^{t_k}; 0 \leq P_{Bdj}^{t_k}; P_{Bcj}^{t_k} \leq 0; \forall t_k \in T \tag{2}$$

$$SOC_{Bj}^{t_k} = SOC_{Bj}^{t_0} - \frac{\varepsilon_{cj}\Delta t}{E_{Bnomj}} \sum_{t=1}^{t_k} P_{Bcj}^{t} - \frac{\Delta t}{E_{Bnomj}\varepsilon_{dj}} \sum_{t=1}^{t_k} P_{Bdj}^{t_k} \tag{3}$$

$$P_{wj}^{t_k} = \delta_w A_w \left(S_w^{t_k}\right)^3 /2; \forall t_k \in T \tag{4}$$

$$P_{CDm}^{t_k}\left(V_{CDm}^{t_k}, I_{CDm}^{t_k}\right) = I_{CDm}^{t_k} V_{CDm}^{t_k}; \forall t_k \in T \tag{5}$$

$$S_{li}^{t_k} = P_{li}^{t_k} + jQ_{li}^{t_k} \forall t_k \in T \tag{6}$$

Symbols and acronyms are not described in this section, but the interested reader can find their meaning in table 1 for symbols and table 2 for acronyms.

2.3. Cost functions: the optimization problem

In this work, the following bi-objective optimization problem is considered:

$$\{\min f_1, \min f_2\} \tag{7}$$

The first cost function, f_1, symbolizes the emissions produced by the fossil fuels used in the main grid for power generation. CO_2 equivalents are considered for traditional generators and diesel generation. The emissions caused by the photovoltaic system, wind turbine, and batteries are considered zero. Equation 8 expresses mathematically this objective function.

$$f_1 = \sum_{t_k=1}^{N_p} \sum_{j=1}^{N_b} \chi_j \left(P^{t_k}\right) \tag{8}$$

where N_b is the number of connecting nodes, χ_j represents the emission factor of each connecting node, P (including the main grid, the diesel generator, the solar system, the wind system, and the batteries) at time t_k. According to the Environmental Protection Agency (EPA), the emission factor values are the upper limits of CO_2 emissions [25].

The second cost function, f_2, represents the cost of energy (see Equation 9). It is calculated based on the cost of the fuel spent to generate electricity using the distributed energy resources included in the microgrid, and the cost of maintenance. Renewable energy sources, such as solar and wind, are assumed to have a maintenance cost, but no fuel operating costs. Mathematically, it can be written as:

$$f_2 = \sum_{t_k=1}^{N_p} \sum_{j=1}^{N_b} a_j + b_j \left(P_{DG_j}^{t_k}\right) + c_j \left(P_{MG_j}^{t_k}\right)^2 \tag{9}$$

where the parameters a, b, and c are the generation cost coefficients in €/kW. Finally, P_{MG} and P_{DG} are the generation output power of the main grid and the power of the diesel generator, respectively, both in kW [26].

Our bi-objective problem has also several constraints that must be satisfied. Equation (10) represents the equality constraints, which indicates the microgrid's active and reactive power balance. More precisely, the first part of the equation (10) represents the active power balance, while the second part describes the microgrid's reactive power balance, and the third block of the photovoltaic system model [27].

$$\boldsymbol{h}^{t_k}\left(\boldsymbol{x}^{t_k}\right) = \left\{ \begin{array}{c} P_{MGj}^{t_k} + P_{DGj}^{t_k} + \sum_{\forall j} P_{Bcj}^{t_k} + \sum_{\forall j} P_{Bdj}^{t_k} + \sum_{\forall j} P_{wj}^{t_k} + \\ \sum_{\forall j \in i} P_{CDj}^{t_k} - \sum_{\forall j \in i} P_{lj}^{t_k} - \sum_{\forall j \in i | j \in N_{Al}, N_T} P_{injj}^{t_k}(\boldsymbol{V}, \boldsymbol{\theta}) = 0, \\ Q_{MGj}^{t_k} - \sum_{\forall j} Q_{lj}^{t_k} - \sum_{\forall j}^{t_k} Q_{injj}(\boldsymbol{V}, \boldsymbol{\theta}) = 0 \\ j = 1, 2, \ldots, N_{bAC}; = 1, 2, \ldots, N_{bAC} \mid \forall j \notin N_{GEN} \\ \Delta I_{CDm}^{t_k} = I_{CDm}^{t_k} - f_{CD}\left(V_{CDm}^{t_k}, I_{CDm}^{t_k}\right) = 0, \\ \Delta P_{CDm}^{t_k} = P_{ACm}^{t_k}(\boldsymbol{V}, \boldsymbol{\theta}) - \Delta P_{CDm}^{t_k}\left(V_{CDm}^{t_k}, I_{CDm}^{t_k}\right) = 0 \\ \Delta V_{CDm}^{t_k} = V_{CDm}^{t_k} - \left(\frac{\pi}{16}\right) V_m^{t_k} = 0 \\ m = N_{bAC} + 1, \ldots, N_{bAC} + N_{bCD} \end{array} \right\} \forall t_k \in T \tag{10}$$

Some inequality constraints have also been taken into consideration. Equation (11) represents the interval $[SOC_{Bj}^{min}, SOC_{Bj}^{max}]$, where the SOC of the batteries must be included [28]. Equation (12) represents the inequality constraints to a variable that indicates the maximum and minimum values of voltage, frequency, and power of the microgrid components.

$$\boldsymbol{z}^{t_k}\left(\boldsymbol{x}^{t_k}\right) = \left\{SOC_{Bj}^{\min} \leq SOC_{Bj}^{t_k} \leq SOC_{Bj}^{\max}\right\} \forall j \in N_B, \forall t_k \tag{11}$$

$$\left\{\begin{array}{c} \underline{\boldsymbol{y}}_{MG} \leq \boldsymbol{y}_{MG}^{t_k} \leq \overline{\boldsymbol{y}}_{MG} \\ \underline{\boldsymbol{y}}_{CD} \leq \boldsymbol{y}_{CD}^{t_k} \leq \overline{\boldsymbol{y}}_{CD} \\ \underline{\boldsymbol{y}}_{B} \leq \boldsymbol{y}_{B}^{t_k} \leq \overline{\boldsymbol{y}}_{B} \\ \underline{\boldsymbol{y}}_{W} \leq \boldsymbol{y}_{W}^{t_k} \leq \overline{\boldsymbol{y}}_{W} \\ \underline{\boldsymbol{y}}_{DG} \leq \boldsymbol{y}_{DG}^{t_k} \leq \overline{\boldsymbol{y}}_{DG} \end{array}\right\} \forall t_k \in T \tag{12}$$

Once the optimization problem is defined, both common multi-objective terminology and what it means to solve a multi-objective problem (MOP) are explained.

Definition 2.1. *For two feasible vectors* $\mathbf{x}, \mathbf{x}' \in S$*, we say that* $\mathbf{x}$ dominates $\mathbf{x}'$ *and* $\mathbf{f}(\mathbf{x})$ *dominates* $\mathbf{f}(\mathbf{x}')$ *if and only if* $f_i(\mathbf{x}) \leq f_i(\mathbf{x}')$ *for all* $i = 1, \ldots, m$*, and there exists one* $j \in \{1, \ldots, m\}$ *such that* $f_j(\mathbf{x}) < f_j(\mathbf{x}')$*.*

Definition 2.2. *A decision vector* $\mathbf{x} \in S$ *is said to be* efficient *or* a Pareto optimal solution *if and only if there does not exist another feasible vector* $\mathbf{x}' \in S$ *dominating* $\mathbf{x}$*, i.e., none of the objective functions can be improved without worsening at least one of the others. The set* S_E *of all the Pareto optimal solutions is called the* efficient set *or the* Pareto optimal set*. The image of a Pareto optimal solution* $\mathbf{f}(\mathbf{x})$ *is called* Pareto optimal objective vector *and the set of all the Pareto optimal objective vectors* $\mathbf{f}(S_E)$ *is denominated* Pareto optimal front*.*

Therefore, solving an MOP as formulated in Equation (7) means obtaining the whole non-dominated subset formed by all the efficient decision vectors, whose corresponding objective vectors represent the Pareto optimal front. Nevertheless, for most MOPs, obtaining an accurate description of the efficient set (or PF) is not possible because those sets are usually a continuum and include an infinite number of points. Furthermore, the computing cost may be high, which is an essential issue for hard-to-solve optimization problems, such as the one considered here.

This work proposes using heuristic multi-objective optimization algorithms (MOEAs), which obtain 'good approximations' of the PF in reasonable computing times. A suitable *PF approximation* (PFA) as a finite set of non-dominated objective vectors which cover the whole PF evenly (see Figure 1) is defined. Notice that the extreme points corresponds to the solutions that minimize f_1 and f_2.

2.4. Optimizer

To solve the optimization problem previosly defined, the multi-objective genetic algorithm (GA) **gamultiobj** provided by the MatLab® toolbox has been chosen [29].

Genetic algorithms search for the solution of a function by employing procedures that mimic the natural evolution, that is, by using operations such as crossover, mutation, and selection that are applied to individuals (candidate solutions) in a population [30]. These mechanisms are executed from an initial population until a termination criterion is satisfied [31].

Crossing over takes two individuals and produces two new ones, while mutation alters one individual to create a single new solution. In this work, a crossover heuristic that penalizes the crossover between candidate solutions that are too similar is used; this encourages diversity in the population and helps prevent premature convergence towards a less than optimal solution. In addition, Adaptive Feasible Mutation is considered, this mutation strategy randomly chooses an improvement direction and a step length, and moves a candidate solution whenever the objective function value increases and the constraints are satisfied [32].

The selection of individuals to produce successive generations plays a vital role in a genetic algorithm. In this paper, the @selectiontournament tool has been considered [33], which is a probabilistic method based on the fitness of the individual, so that the best individuals have a higher probability of being selected. In our implementation, an individual in the population cannot be selected more than once, and all individuals in the population have the possibility of being selected and be part of the next generation.

The initial population considered here is composed of 100 individuals randomly created, which evolve during the optimization procedure until a stopping criterion is satisfied, i.e. after 5000 generations are achieved.

As a result of the multi-objective optimization algorithm, a PF approximation is obtained. Then, there are available a set of points that are individually satisfactory solutions.

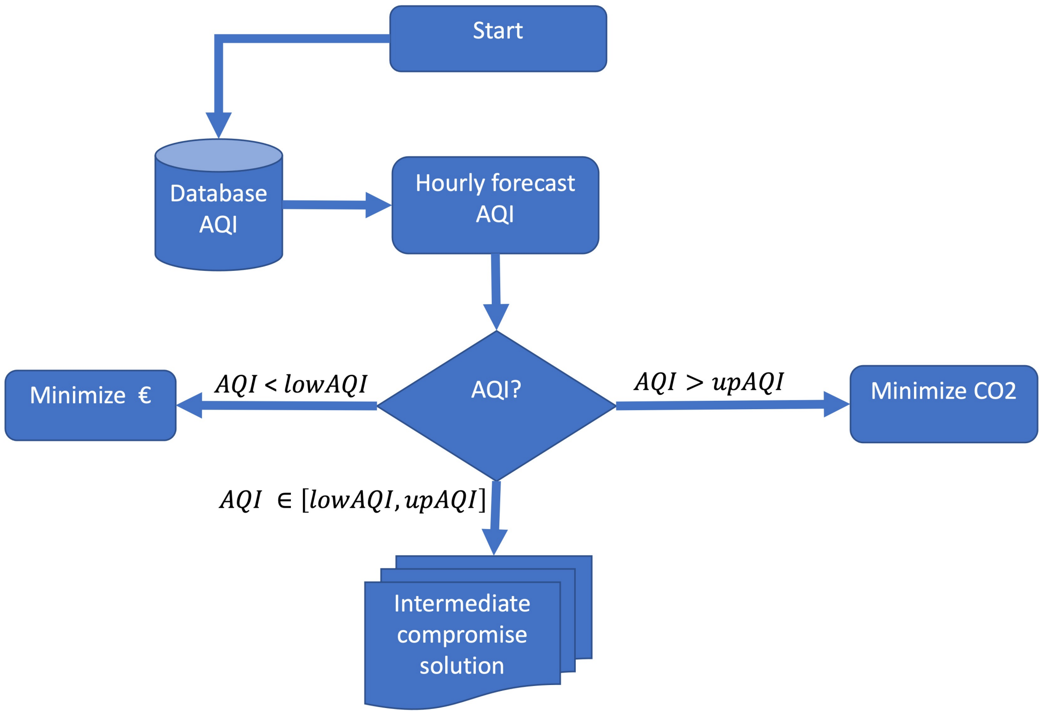

Figure 3: Decision tool flow chart.

2.5. Decision-tool

In this work, an online decision tool (DT) to select the preferable solution according to pre-specified criteria is proposed. See Figure 3 for a graphical representation. In particular, the designed decision scheme will choose, among the points that compose the PF, the one minimizing the CO_2 whether the Air Quality Index (AQI) is higher than a given threshold $upAQI$. Similarly, it will choose the solution minimizing the cost of energy if the AQI is lower than an established boundary $lowAQI$. Notice that those points are the extreme points of the PF, depicted in yellow and green colors in Figure **??**. For those cases where the air quality stays in the interval $[lowAQI, upAQI]$, the decision tool will select a compromise solution to balance the costs and the emissions of CO_2. Specifically, it will select from the PF the solution that is proportionally away from the minimum distance between the current AQI and the $lowAQI$ and $upAQI$ boundaries.

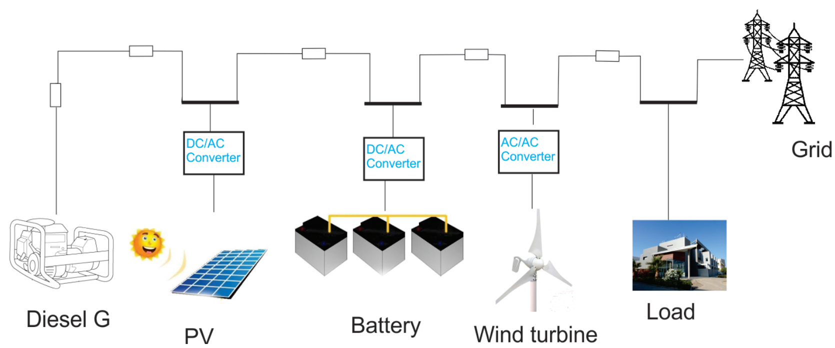

Figure 4: Scheme of the microgrid test.

3. Results and discussion

This section summarizes the simulation framework where the experiments have been carried out as well as the obtained results.

3.1. Testbed description for simulation

The microgrid considered as a testbed is located in the CIESOL bioclimatic building at the University of Almería (Spain). Broadly speaking, a bioclimatic building is a type of building design that takes into account the local climate to minimize the use of artificial heating and cooling systems. This is achieved by utilizing natural ventilation, thermal mass, and other passive design techniques to regulate the temperature and airflow within the building and, in this way, the thermal comfort of its users. A bioclimatic building can include renewable energy systems such as solar panels, wind turbines, and geothermal systems to generate electricity and provide heating and cooling. By integrating these systems with the building's design, a bioclimatic building can become energy-efficient, reduce its carbon footprint, and achieve energy self-sufficiency. In our particular case, the CIESOL's microgrid comprises a storage system (battery), a wind turbine, a diesel generator, a photovoltaic (PV) system connected to the main grid and some loads, see Figure 4. The power that those elements can produce or consume from the microgrid are (all in kW) 2, 1, 3, 2 and 6, respectively.

The data inputs for the microgrid simulation are shown in Figure 5. From top to bottom, it is possible to see: i) the solar radiation profile, ii) the wind speed profile for Almeria and, iii) the load profile of a part of the bioclimatic laboratories of CIESOL. The solid blue line shows the current data, and the dashed red line shows the predictions made by the Double Exponential

Smoothing (DES) method. The DES method consists of performing two exponential smoothings from which a forecast is obtained, in this case, of solar radiation and wind speed. The calculation applies an expression to the values observed in the time series. Then a second expression is made to the attenuated series obtained through the first smoothing [34]. The reader can see that the DES method is able to predict the inputs for the simulation almost without error.

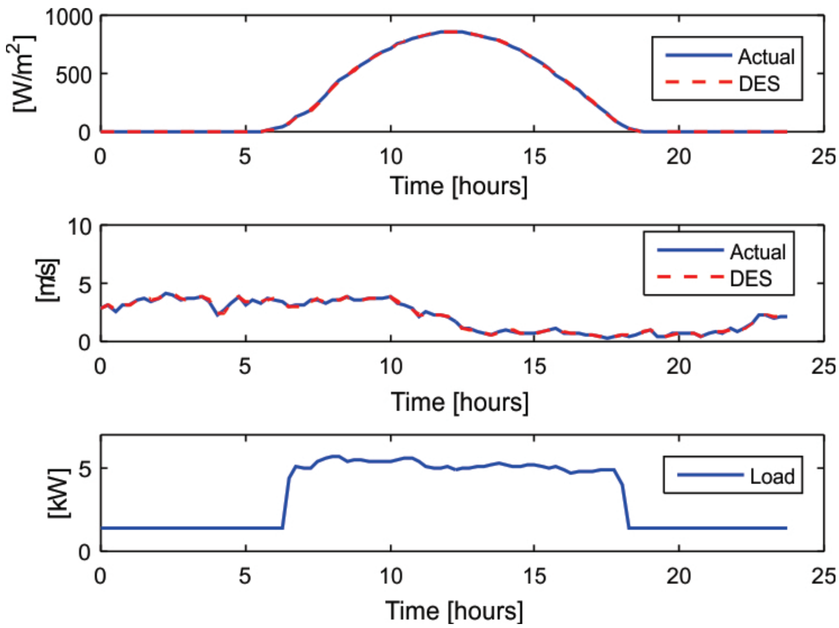

Figure 5: Forecasting curves for the testbed microgrid.

The hourly information of the air quality index is provided by the Ministry for the Ecological Transition and the Demographic Challenge of Spain (MITECO). In particular, the atmospheric measurements of the air quality index of the city of Almería are taken [35]. For the DT, an interval of $[lowAQI, upAQI] = [202, 278]$ μg$/m^3$ has been considered.

To analyze the performance of the proposed EMS, two simulations have been carried out. In the first one, it is considered that there are not prediction errors, while in the second one an error is introduced in the forecasting variables.

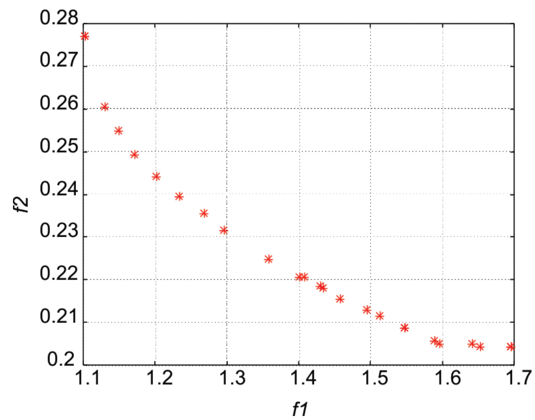

Figure 6: Pareto-front obtained by the multi-objective optimizer when no prediction errors are considered.

.

3.2. Simulation without error in predictions

In this case, several assumptions have been made. In particular, it is assumed that there is no error in the prediction of the forecast variables, see Figure 5. Zero energy cost and CO_2 emission coefficients are used for the PV system, wind system and battery; high cost and low CO_2 emission coefficients are considered for the energy coming from the main grid; low cost and high CO_2 emission coefficients are assigned for the diesel generator; and, finally, a sampling time for the MPC equal to 15 minutes and a prediction horizon of N_p=10 are set, which means that the optimization is performed with prediction variables predicted for the next 2:30 hours. Regarding the multi-objective optimization algorithm, it has been configured to provide at most 25 solutions in the PF.

Figure 6 shows a graphical representation of the PF obtained. According to the scheme shown in Figure 1, that PF will be the input of the decision tool, which will select the preferable solution according to the AQI index and the preferences summarized in subsection 2.5. In the following, we analyze the solution provided by the tool when different values of AQI are considered.

Let us consider the case where the AQI $\geq$ 278 μg/m^3, which indicates that the city has high pollution rates. In this case, the decision tool selects the point that minimizes CO_2 emissions, i.e., the one with values equal to $(f_1, f_2) = (1.10, 0.278)$ and which corresponds to the extreme upper solution in the PF. The results of this simulation are depicted in Figure 7.

As can be seen, the main grid power is mainly used as primary, since it has a lower CO_2 emission coefficient than the diesel generator. It is worth mentioning that, each generation source contributes to supply the microgrid load, represented in the figure by the red solid line. As can be seen, from 00:00 to 8:00 hours, the demand is satisfied by the main grid generation, the wind turbine and the energy saved in the battery. In addition, the surplus from the wind turbine is sometimes used to charge the battery. In the period between 8:01 hours and 18:00 hours, demand is met by the main grid, the photovoltaic system, since these are the hours of highest solar irradiation, the battery and minimally by the diesel generator. In addition, the surplus generated by the PV system contributes to charging the battery. In fact, it mainly supplies the main grid and the battery in the following hours. In general, we can conclude that the solution provided is valuable and satisfies the requirements imposed.

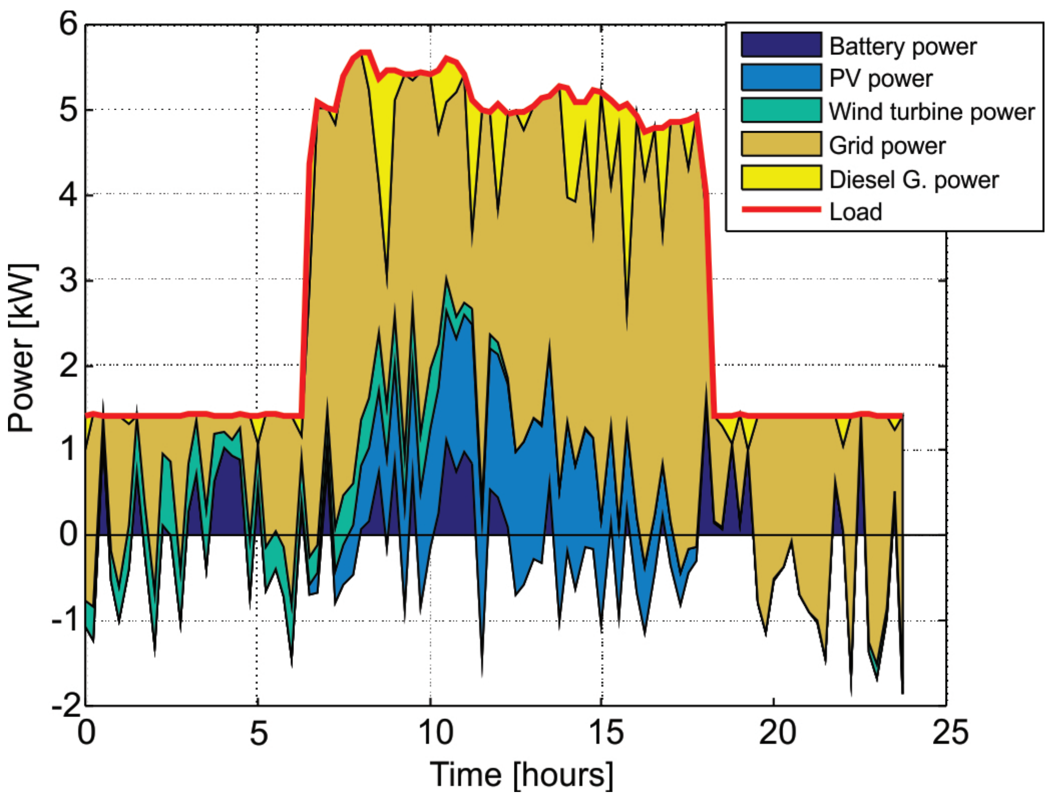

Figure 7: Simulation for the left upper solution of the PF.

Let us now analyze the opposite case, where the city has the lowest pollution rates and the AQI $\leq 202\ \mu g/m^3$. Now, the decision tool selects the point in the lower right corner with values $(f_1, f_2) = (1.69, 0.202)$. A graphical representation of such a solution is given by Figure 8. In this case, the objective is to minimize the economic cost of the microgrid, which explains why the contribution of the diesel generator is greater than that considered in the previous case. Specifically, in the period from 00:00 to 8:00, it begins to contribute to the achievement of the demand.. In the stretch from 8:01 to 18:00 (hours of most significant consumption), the contribution of the diesel generator is the maximum to minimize energy costs in the microgrid. Finally, it should be noted that, at times of high energy production, the battery is charged from renewable sources such as the photovoltaic system and the wind turbine, since these are cheap and non-polluting energies.

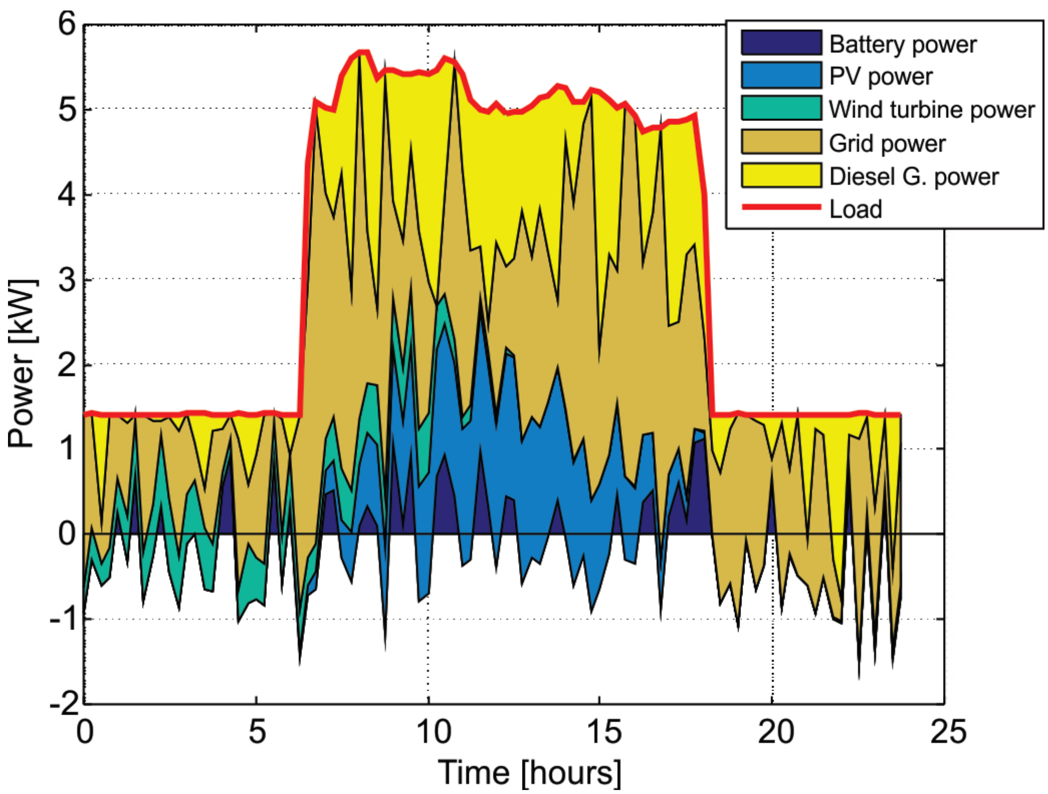

Figure 8: Simulation for the right lower solution of the PF.

Finally, Figure 9 shows the compromise solution chosen by the decision tool for the case where pollution levels are intermediate in the city. It lies right in the middle of the PF $(f_1(x), f_2(x)) = (1.40, 0.222)$. This solution presents a compromise between minimizing energy cost and minimizing CO_2 emissions. It is observed that from 8:00 hours to 18:00 hours, there is an increase in the energy contribution of the diesel generator trying to balance the total energy cost in the microgrid. The contribution of the diesel generator is higher than in the first case (upper left corner of the PF where the minimization of CO_2 emissions has priority) but lower than in the second case (lower right corner of the PF where the economic cost has priority). Data on minimum and maximum pollution levels in Almeria city Council have been provided by the Spanish Ministry for the Ecological Transition and the Demographic Challenge (MITECO).

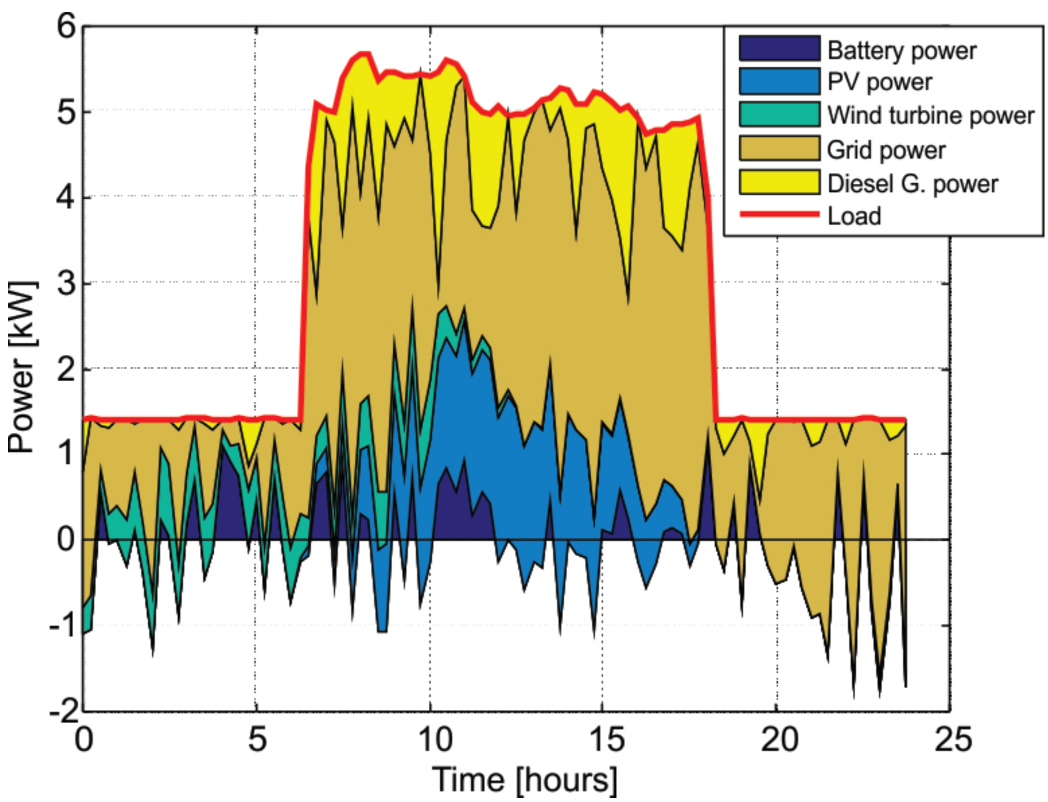

Figure 9: Simulation for a compromise solution in the middle of the PF.

3.3. Simulation with error in predictions

The receding horizon makes the MPC more robust to uncertainties. This is because at each sample time the values of the forecasting variables are updated with new information and the optimization is re-run through the control horizon. However, in other EMS, the optimization is performed only once at the beginning of the simulation, so these uncertainties may be larger.

Then, to evaluate the robustness of the MPC, an error has been added to the prediction of the forecast variables, i.e. solar radiation and wind speed. Specifically, an error of 12% lower than the actual value of the variable has been considered, as is possible to see in Figure 10. This figure gives a graphical representation of the error profile. Notice that this error is time-weighted, i.e., at the beginning of the simulation, time t, the future error for the next sampling time $t+1$ is almost negligible, but as the time horizon of the predictions increases, this error increases significantly. Therefore, as the information of the prediction variables is updated at each sampling time, this error will always be bounded.

Figure 11 shows the new PF obtained for the case in which the 12% error is introduced. As can be seen, there are negligible variations in the PF with respect to the case in which there is no error.

The same three scenarios considered in subsection 3.2 have now been analyzed. More specifically: (i) the solution chosen by the decision tool when the city has the highest pollution rates and the main priority is to reduce CO_2 emission, i.e., the point located in the upper left corner of the PF $(f_1(x), f_2(x)) = (1.187, 0.283)$; ii) the solution chosen when the city has the lowest pollution rates and the priority is to reduce the economic cost, i.e., the point in the lower right corner of the PF $(f_1(x), f_2(x)) = (1.78, 0.210)$, and; iii) a compromise solution between minimizing energy cost and CO_2 emissions, i.e., the midpoint of the PF $(f_1(x), f_2(x)) = (1.486, 0.227)$. The simulation results for these three cases are shown in the top image, the middle image, and the bottom image of Figure 12, respectively.

All simulations have almost the same results as those shown when there is no error in the forecast variables (see Figures 7-9). In fact, the differences are not significant at first glance. These results demonstrate the robustness of the proposed MPC to the uncertainties, which is an advantage over optimizing only once at the beginning of the simulation, since its efficiency could be more affected by the errors of the forecast variables.

Finally, taking into account the efficiency of the proposed approach, it is worth mentioning that in our experiments, the computation time employed

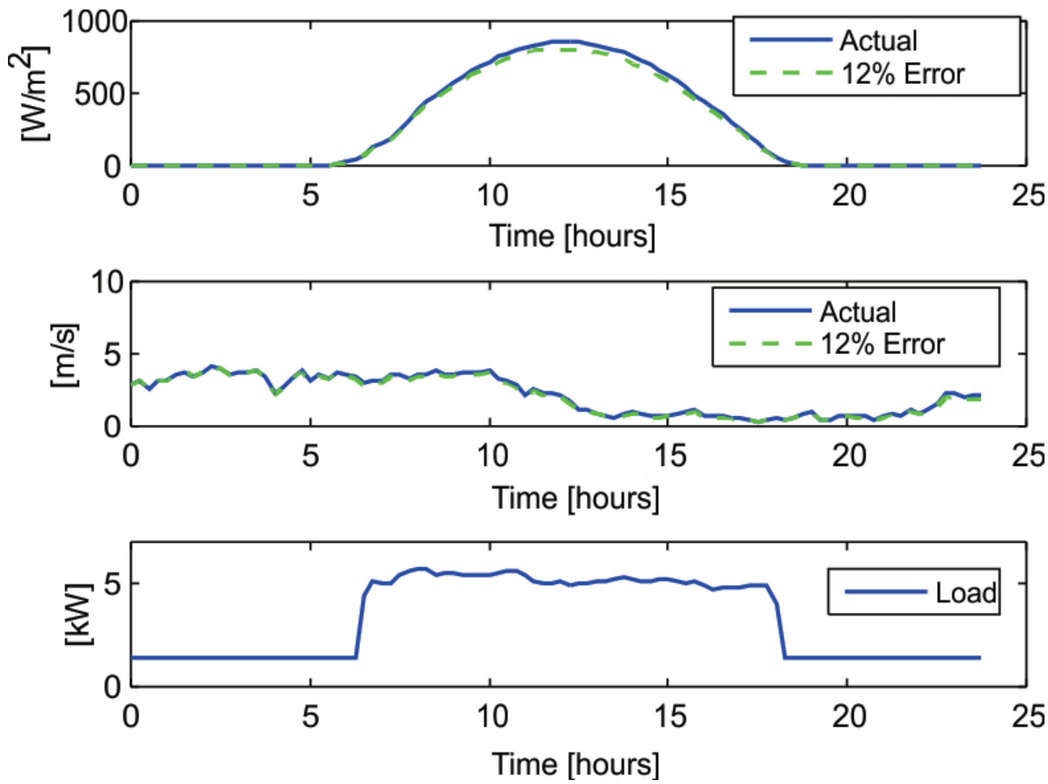

Figure 10: Forecast curves with a twelve per cent error.

by both the multi-objective algorithm and the decision tool to finally select the preferred solution was 1709 seconds. The contribution of the decision tool to this time is practically negligible, which means that the optimization algorithm consumes most of this time.

To illustrate the efficiency of the proposed approach, a small computational experiment has been carried out consisting of replacing the multi-objective algorithm by a single-objective one and then running two experiments in which the functions $f_1(x)$ and $f_2(x)$ are independently minimized. For this purpose, we considered the genetic algorithm (GA) included in the Matlab Global Optimization Toolbox configured to consume the same number of function evaluations as the multi-objective method. Thus, the comparison is fair since both algorithms have the same budget to reach the optima.

Table 3 summarizes the values of the objective functions obtained and the computation time consumed by the GA. In addition, for comparison, we have evaluated the solution obtained when $f_1(x)$ is minimized, with the func-

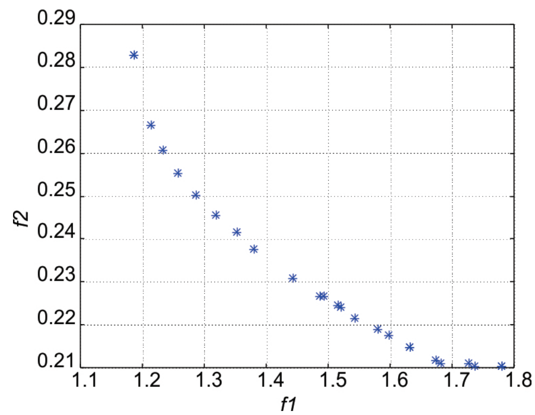

Figure 11: Pareto-front obtained by the multi-objective optimizer when prediction errors are considered.

tion $f_2(x)$, and vice versa. This calculation is highlighted in the table with a "*", warning that this results from evaluating the optimal solution found with the other objective function. In addition, for the reader's convenience, we have also included the results of the multi-objective algorithm. Specifically, we have included the total time consumed and the objective function values associated with the Pareto front endpoints. Notice that those two solutions correspond to the solutions that minimize $f_1(x)$ and $f_2(x)$, respectively. Hence, they are comparable in terms of effectiveness with the ones obtained by the GA. As can be seen, solutions of similar quality are obtained for the single-objective and multi-objective algorithms, meaning that both are comparable in terms of effectiveness.

From an efficiency point of view, the multi-objective algorithm used 1709 seconds to obtain 25 different compromised solutions in a single run, including those obtained by the single-objective problems. In contrast, with a single-objective methodology, every time the problem conditions change, another optimization problem needs to be solved. Then, the single-objective algorithm required 2511 seconds and two independent runs to obtain only two solutions, demonstrating that the multi-objective approach outperforms the single-objective approach in terms of computational complexity.

4. Conclusions

The transition in the electricity markets between the traditional electricity generation model and a new model in which electricity will be generated in a distributed manner through microgrids, will only be possible with the development of efficient energy management systems.

This work takes a step in that direction and presents an EMS capable of satisfying the energy demand while considering requirements regarding allowable CO_2 emissions and energy cost. More specifically, the EMS can adapt to frequently changing operating conditions and automatically consider a solution that minimizes CO_2 emissions, energy costs or a compromise solution between the two. To do so, the EMS includes three components: an MPC that makes the EMS more robust to uncertainties; a multi-objective algorithm that allows optimizing more than one objective simultaneously and proposes several candidate solutions; and a decision tool that selects the most appropriate solution for the current scenario.

To illustrate how MPC helps to increase the robustness and performance of the proposed EMS, we conducted a study in which no prediction errors were considered and another in which the prediction failed. The results showed that thanks to the decreasing horizon feature, the MPC could correct the erroneous predictions and provide a solution of equal quality to the one obtained when the prediction was correct.

Moreover, to show the benefits of using both the multi-objective optimization and the decision tool, several solutions from the PF were analyzed. The experiments showed that different candidate solutions could be obtained in a single optimization run. The decision tool was responsible for selecting the most suitable one based on the implemented preferences.

Therefore, it can be concluded that the proposed EMS is a promising tool for managing the energy flows in the microgrid.

In the future, we plan to extend the problem to more than two objectives and test other multi-objective techniques, such as those based on preferences.

Acknowledgments

This work has been financed by CONACYT-Mexico under Project 2015-01-786 (Problemas Nacionales) and by the National R+D+i Plan Projects PID2021-123278OB-I00 and PID2021-126889OB-I00 of the Spanish Ministry of Science and Innovation and EIE funds.

Declaration of Interests

The authors declare that they have no known competing financial interests or personal relationships that could have appeared to influence the work reported in this paper.

References

[1] Eurostat, Eurostat - statistics explained, https://ec.europa.eu/eurostat/statistics-explained/index.php, last access: 30^{th}, September 2022 (2022).

[2] BP, bp - statistical review of world energy, https://www.bp.com/en/global/corporate/energy-economics/statistical-review-of-world-energy.html, last access: 30^{th}, September 2022 (2022).

[3] M. Yaghi, F. Luo, H. E. Fouany, L. Junfeng, H. Jiajian, Z. Jun, Multi-objective optimization for microgrid considering demand side management, in: 2019 Chinese Control Conference (CCC), 2019, pp. 7398–7403. doi:10.23919/ChiCC.2019.8865498.

[4] D. Fioriti, S. Pintus, G. Lutzemberger, D. Poli, Economic multi-objective approach to design off-grid microgrids: A support for business decision making, Renewable Energy 159 (2020) 693–704. doi:https://doi.org/10.1016/j.renene.2020.05.154.
URL https://www.sciencedirect.com/science/article/pii/S0960148120308594

[5] T. Schmitt, T. Rodemann, J. Adamy, Multi-objective model predictive control for microgrids, at - Automatisierungstechnik 68 (8) (2020) 687–702. doi:doi:10.1515/auto-2020-0031.
URL https://doi.org/10.1515/auto-2020-0031

[6] H. Chen, L. Gao, Z. Zhang, Multi-objective optimal scheduling of a microgrid with uncertainties of renewable power generation considering user satisfaction, International Journal of Electrical Power and Energy Systems 131 (2021) 107142. doi:https://doi.org/10.1016/j.ijepes.2021.107142.
URL https://www.sciencedirect.com/science/article/pii/S0142061521003811

[7] U. R. Nair, R. Costa-Castelló, An analysis of energy storage system interaction in a multi objective model predictive control based energy management in dc microgrid, in: 2019 24th IEEE International Conference on Emerging Technologies and Factory Automation (ETFA), 2019, pp. 739–746. doi:10.1109/ETFA.2019.8869474.

[8] I. V., L. R., S. V., V. V., P. Siarry, L. Uden, Multi-objective optimization and energy management in renewable based ac/dc microgrid, Computers and Electrical Engineering 70 (2018) 179–198. doi:https://doi.org/10.1016/j.compeleceng.2018.01.023.
URL https://www.sciencedirect.com/science/article/pii/S0045790617301283

[9] D. Fioriti, G. Lutzemberger, D. Poli, P. Duenas-Martinez, A. Micangeli, Coupling economic multi-objective optimization and multiple design options: A business-oriented approach to size an off-grid hybrid microgrid, International Journal of Electrical Power & Energy Systems 127 (2021) 106686. doi:10.1016/j.ijepes.2020.106686.

[10] M. B. Shadmand, R. S. Balog, Multi-objective optimization and design of photovoltaic-wind hybrid system for community smart dc microgrid, IEEE Transactions on Smart Grid 5 (5) (2014) 2635–2643. doi:10.1109/TSG.2014.2315043.

[11] G. Aghajani, N. Ghadimi, Multi-objective energy management in a micro-grid, Energy Reports 4 (2018) 218–225. doi:https://doi.org/10.1016/j.egyr.2017.10.002.
URL https://www.sciencedirect.com/science/article/pii/S2352484717301154

[12] X. Zhang, R. Sharma, Y. He, Optimal energy management of a rural microgrid system using multi-objective optimization, in: 2012 IEEE PES Innovative Smart Grid Technologies (ISGT), 2012, pp. 1–8. doi:10.1109/ISGT.2012.6175655.

[13] S. Bechikh, R. Datta, A. Gupta (Eds.), RMulti-Objective Optimization Problems, Vol. 1 of SpringerBriefs in Mathematics, Springer, 2017. doi:10.1007/978-3-319-58565-9.
URL https://doi.org/10.1007/978-3-319-58565-9

[14] M. R. Ferrández, J. L. Redondo, B. Ivorra, A. M. Ramos, P. M. Ortigosa, B. Paechter, Improving the performance of a preference-based multi-objective algorithm to optimize food treatment processes, Engineering Optimization 52 (5) (2020) 896–913. doi:10.1080/0305215X.2019.1618289.

[15] S. Puertas-Martín, J. Redondo, M. Ferrández, H. Pérez-Sánchez, P. Ortigosa, Multipharm-dt: A multi-objective decision tool for ligand-based virtual screening problems, Informatica 33 (1) (2021) 55–80. doi:10.15388/21-INFOR469.

[16] O. Gonzales Zurita, J.-M. Clairand, E. Peñalvo-Lopez, G. Escriva Escriva, Review on multi-objective control strategies for distributed generation on inverter-based microgrids, Energies 13 (13) (2020). doi:10.3390/en13133483.
URL https://www.mdpi.com/1996-1073/13/13/3483

[17] H. R. A.-H. Bouchekara, M. S. Shahriar, M. S. Javaid, Y. A. Sha'aban, M. A. M. Ramli, Multi-objective optimization of a hybrid nanogrid/microgrid: Application to desert camps in hafr al-batin, Energies 14 (5) (2021). doi:10.3390/en14051245.
URL https://www.mdpi.com/1996-1073/14/5/1245

[18] A. L. Bukar, C. W. Tan, L. K. Yiew, R. Ayop, W.-S. Tan, A rule-based energy management scheme for long-term optimal capacity planning of grid-independent microgrid optimized by multi-objective grasshopper optimization algorithm, Energy Conversion and Management 221 (2020) 113161. doi:https://doi.org/10.1016/j.enconman.2020.113161.
URL https://www.sciencedirect.com/science/article/pii/S0196890420307056

[19] S. Bechikh, R. Datta, A. Gupta (Eds.), Recent Advances in Evolutionary Multi-objective Optimization, Vol. 20 of Adaptation, Learning, and Optimization, Springer, 2017. doi:10.1007/978-3-319-42978-6.
URL https://doi.org/10.1007/978-3-319-42978-6

[20] Q. Zhang, J. Ding, W. Shen, J. Ma, G. Li, Multiobjective particle swarm optimization for microgrids pareto optimization dispatch, Mathematical Problems in Engineering 2020 (2020).

[21] X. Li, Z. Li, Micro-grid resource allocation based on multi-objective optimization in cloud platform, in: 2017 8th IEEE International Conference on Software Engineering and Service Science (ICSESS), 2017, pp. 509–512. doi:10.1109/ICSESS.2017.8342966.

[22] B. Hong, Z. Zheng, Stochastic multi-objective dynamic optimal dispatch for combined heat and power microgrid, in: 2016 IEEE PES Asia-Pacific Power and Energy Engineering Conference (APPEEC), 2016, pp. 2369–2373. doi:10.1109/APPEEC.2016.7779908.

[23] E. F. Camacho, C. B. Alba, Model predictive control, Springer science & business media, 2013.

[24] A. Gholami, M. Ameri, M. Zandi, R. Gavagsaz Ghoachani, A single-diode model for photovoltaic panels in variable environmental conditions: Investigating dust impacts with experimental evaluation, Sustainable Energy Technologies and Assessments 47 (2021) 101392. doi:https://doi.org/10.1016/j.seta.2021.101392.
URL https://www.sciencedirect.com/science/article/pii/S2213138821004021

[25] A. Kamboj, S. Chanana, Optimization of cost and emission in a renewable energy micro-grid, in: 2016 IEEE 1st International Conference on Power Electronics, Intelligent Control and Energy Systems (ICPEICES), 2016, pp. 1–6. doi:10.1109/ICPEICES.2016.7853085.

[26] V. S. Tabar, M. A. Jirdehi, R. Hemmati, Energy management in microgrid based on the multi objective stochastic programming incorporating portable renewable energy resource as demand response option, Energy 118 (2017) 827–839. doi:https://doi.org/10.1016/j.energy.2016.10.113.
URL https://www.sciencedirect.com/science/article/pii/S0360544216315596

[27] D. P. e Silva, J. L. Félix Salles, J. F. Fardin, M. M. Rocha Pereira, Management of an island and grid-connected microgrid using hybrid economic model predictive control with weather data, Applied Energy 278 (2020) 115581. doi:https://doi.org/10.1016/j.apenergy.2020.115581.

URL https://www.sciencedirect.com/science/article/pii/S0306261920310916

[28] E. Sortomme, M. A. El-Sharkawi, Optimal power flow for a system of microgrids with controllable loads and battery storage, in: 2009 IEEE/PES Power Systems Conference and Exposition, 2009, pp. 1–5. doi:10.1109/PSCE.2009.4840050.

[29] Mathworks, Genetic algorithm and direct search toolbox, url=https://es.mathworks.com/help/gads/gamultiobj.html, last access: 30^{th}, September 2022 (2022).

[30] Z. Michalewicz, Evolutionary Programming and Genetic Programming, Springer Berlin Heidelberg, Berlin, Heidelberg, 1996, pp. 283–287. doi:10.1007/978-3-662-03315-9_14.
URL https://doi.org/10.1007/978-3-662-03315-9_14

[31] J. Joines, C. Houck, On the use of non-stationary penalty functions to solve nonlinear constrained optimization problems with ga's, in: Proceedings of the First IEEE Conference on Evolutionary Computation. IEEE World Congress on Computational Intelligence, 1994, pp. 579–584 vol.2. doi:10.1109/ICEC.1994.349995.

[32] C. Houck, J. Joines, M. Kay, A genetic algorithm for function optimization: A matlab implementation, NCSUIE-TR-95-09. North Carolina State University, Raleigh, NC, USA 22 (05 1998).

[33] D. E. Goldberg, Genetic Algorithms in Search, Optimization and Machine Learning, 1st Edition, Addison-Wesley Longman Publishing Co., Inc., USA, 1989.

[34] B. Taghezouit, F. Harrou, Y. Sun, A. H. Arab, C. Larbes, A simple and effective detection strategy using double exponential scheme for photovoltaic systems monitoring, Solar Energy 214 (2021) 337–354. doi:https://doi.org/10.1016/j.solener.2020.10.086.
URL https://www.sciencedirect.com/science/article/pii/S0038092X2031152X

[35] B. Cayir Ervural, R. Evren, D. Delen, A multi-objective decision-making approach for sustainable energy investment

planning, Renewable Energy 126 (2018) 387–402. doi:https://doi.org/10.1016/j.renene.2018.03.051.
URL https://www.sciencedirect.com/science/article/pii/S0960148118303628